

# Advanced Technologies, Materials and Coatings Developed in Scientific-Educational Center of SHS

By E. A. Levashov<sup>1</sup>, A. G. Merzhanov<sup>2</sup> and D. V. Shtansky<sup>1</sup>, Moscow

## 1 History of SHS Center

20 years ago, according to order-decision number 744/119 of September 21, 1989 by the State Committee on Education and Presidium of the Academy of Science of USSR, the Scientific-Educational Center of *SHS MISIS - ISMAN (SHS-Center)* has been established in order to launch scientific integration of the State Technological University *Moscow Institute of Steel and Alloys (MISIS)* and the *Institute of Structural Macrokinetics and Material Science Problems of Russian Academy of Science (ISMAN)* in the field of *Self-Propagating High-Temperature Synthesis (SHS)*. This order-decision determined functions and tasks, statute and structure of the *SHS-Center*. Idea of *SHS-Center* establishment was positively accepted by representatives of State Committee on Education (*Prof. Gennady Yagodin*) and Academy of Science (Academician *Guriy Marchyuk*) of USSR.

Academician *Alexander Merzhanov* (founder of *SHS* and *ISMAN*) and *Prof. Nikolay Khavsky* (vice rector of *MISIS* at those period) were initiators of decision to establish firstly in USSR the *SHS-Center* on the base of both institutes integration. *Prof. Inna Borovinskaya* and *Prof. Nikolay Khavsky* were former scientific leaders. *Dr. Evgeny Levashov* (at present – Professor, Honor Doctor of Colorado School of Mines, Head of the Department of Powder Metallurgy and Functional Coatings of *MISIS*) is a first and present head of the *SHS-Center*.

Nowadays the *SHS-Center* is a multidisciplinary scientific-educational center with a wide area of scientific activity: *SHS*, mechanical activation assisted *SHS (MA SHS)*, physics of combustion, structural macrokinetic, material science of ceramics, intermetallics, composites and functionally graded materials, nanostructured materials, hard-wear-corrosion-heat-resistant coatings, biocompatible thin films and

coatings, nanodispersion strengthened coatings, surface engineering technologies i.e. magnetron sputtering, ion implantation, ion implantation assisted magnetron sputtering, pulse electrospark deposition (*PED*), chemical reaction assisted *PED (CRAPED)*, attestation of mechanical and tribological properties and metrology of nanostructured surfaces.

Every year educational activity includes graduate training in following courses: *Physical-Chemical and Technological Principles of Synthesis of Inorganic Materials in Combustion Regime, Structural Macrokinetics, Technologies of SHS*. Education and training of postgraduate students is achieved by their involvement in the research and development programs. Training also carries out in the frame of *VINF (Virtual Institute of Nanostructured Films)* (<http://www.vinf.eu> of *EXCELL FP6* project). 27 staffs including 4 Dr. Sc. and Professors, 9 PhD and Assoc. Prof., 14 engineers and technicians, 6 post-graduates, 12 students are working now in *SHS-Center*. In the last two decades the *SHS-Center* has been awarded by a number of international awards in the field of *SHS* and surface engineering: *CRDF, INTAS, NATO-Russia, EUREKA, ISTC, UK Royal Society, FP6, FP7*.

The expertise and research leadership of *SHS-Center* is evidenced by above 600 publications on mentioned fields of expertise in referees national and international journals, books, proceedings, and multiple patents and *know-how* on the technologies. The team of *SHS-Center* collaborates with leading research centres in the USA, Europe, Asia, and Japan.

Staffs of *SHS-Center* are members of International Association on *SHS (SHS-AS)*, Int. Committee on *SHS*, European Joint Committee for Plasma and Ion Surface Engineering *EJC/PISE*, International Advisory Committee of *FGM*, Int. Committee on Plasma Surface Engineering, Int. Committee on Metallurgical Coatings and Thin Films, Int. Committee of World Ceramic Congress *CIMTEC*. The *SHS-Center* is a current member of the Advanced Coatings and Surface Engineering Laboratory (*ACSEL*) at the Colorado School of Mines.

<sup>1</sup> State Technological University "Moscow Institute of Steel and Alloys", SHS-Center MISIS-ISMAN, Leninsky pr., 4, Moscow 119049, Russia; e-mail: levashov@shs.misis.ru

<sup>2</sup> Institute of Structural Macrokinetics and Materials Science Problems of Russian Academy of Science, Chernogolovka, Moscow Region, 142432; e-mail: isman@ism.ac.ru

Head of the *SHS-Center Prof. E. A. Levashov* is a editor-in-chief of *Journal Non-Ferrous Metals* – English issue of Russian Journals *Izvestiya Vuzov. Tsvetnaya Metallurgiya* (<http://nmt.msisa.ru/>), *Izvestiya Vuzov. Poroshkovaya Metallurgiya i Funkcionalnie Pokritiya* (<http://pm.msisa.ru/>) and a member of editorial boards of *International Journal of Self-Propagating High-Temperature Synthesis* and *Physical Surface Engineering Journal*.

## 2 Activities of SHS-Center

### 2.1 Advanced Materials

- Composite, Intermetallides and Functionally-Graded Materials (FGM)
- Multicomponent Nanostructured Thin Films and Coatings
- Hard and Ultra-hard
- Wear-Corrosion- and Heat-resistant
- Multilayer Films for Thermal Generators
- Multicomponent Biocompatible Nanostructured Coatings (MUBINAF) for Medicine
- Self-lubricating Coatings
- Bulk Nanostructured Ceramics and Nanodispersion Strengthened Materials and Coatings
- Diamond-Containing FGM and Coatings, Diamond Tools
- Refractory Ceramics

### 2.2 Advanced Technologies

- Self-Propagating High-Temperature Synthesis (SHS), MA SHS
- Powder Metallurgy
- Magnetron Sputtering
- Ion Implantation
- Ion Implantation Assisted Magnetron Sputtering (IIAMS)
- PED and CRAPED

### 2.3 Characterization and Testing Methods

- Characterization of Multicomponent Materials and Nanostructured Coatings Using X-Ray Diffraction, TEM, HRTEM, SEM, AES, SIMS, AFM, and XPS methods.
- Evaluation of Chemical, Thermal, Mechanical and Tribological Properties of Materials and Coatings on Micro- and Nanoscale Using Nanohardness

Tester, Scratch and Impact Testers, Tribometers, Optical Profiling Systems, Complete System for Electrochemical Research, Microcalorimeter, Wetting Angle Measurement System, Optical Emission Spectrometers.

## 2.4 Knowledge, Novel Technologies and Materials

The *SHS-Center* pioneered following knowledge, novel technologies and materials:

- Theoretical model for thermal and chemical combustion wave propagation in multilayer system was developed;
- Structural and thermal inhomogeneity of combustion zone because of powder mixture heterogeneity was fixed on microlevel using a high speed video movie;
- It was established the theoretical model of *concurrent infiltration* for combustion process in capillary porous systems containing reagent and inert melts;
- Scientific and technological principles of *SHS* in solid-liquid, liquid-liquid, and solid-gas systems affected by ultrasonic fields were created;
- *MA SHS* was applied in order to realize the combustion process in low exothermal mixtures. Convenient method for approximated estimation of MA contribution to change of activation energy of combustion process by measurement of heat evolution rate of exothermic mixtures before and after MA was suggested. Technological regimes of MA for green mixtures in systems Ti-Si, Mo-Si, Ti-Cr-C, Ti-B, Ti-BN, Ti-Si<sub>3</sub>N<sub>4</sub>, Ti-Cr-B, Cr-B, Mo-B, Mo-Si, Ti-Ta-C, Ni-Al, Ti-Cr-Al-C were optimized;
- *SHS*-technology of composite targets production (for example, TiC-TiB<sub>2</sub>, TiB<sub>2</sub>-Al<sub>2</sub>O<sub>3</sub>, TiC $\alpha$ , TiB<sub>2</sub>-Ti<sub>5</sub>Si<sub>3</sub>, TiB-Ti, TiN-TiB<sub>2</sub>, TiN-Ti<sub>5</sub>Si<sub>3</sub>, TiC-Ti<sub>3</sub>SiC<sub>2</sub>-TiSi<sub>2</sub> (SiC), TiB<sub>2</sub>-TiAl, TiC-Cr<sub>3</sub>C<sub>2</sub>, TiC-TiAl, Ti<sub>5</sub>Si<sub>3</sub>-Ti, TiB<sub>2</sub>-CrB<sub>2</sub>, CrB<sub>2</sub>, (Ti,Mo)C-Mo<sub>2</sub>C, TiC-TaC-Mo<sub>2</sub>C, TiC $\alpha$ -CaO(ZrO<sub>2</sub>), TiC $\alpha$ -Ca<sub>3</sub>(PO<sub>4</sub>)<sub>2</sub>, (Ti,Ta)C $\alpha$ -Ca<sub>10</sub>(PO<sub>4</sub>)<sub>6</sub>(OH)<sub>2</sub> and many others) for magnetron sputtering of nanostructured multifunctional coatings was developed and implemented in practice;
- *SHS*-technology of diamond containing composites production including *FGMs* under research program in cooperation with *Tomei Diamond Co., Ltd.* and Ryukoky University was developed;

- Innovative approach to manufacturing lines of diamond containing segments production for cutting wheel and drills for build industry and stone treatment which was developed recently. Nano-sized additives to metallic binder are used in order to improve in 2 to 3 times a working ability and service life of diamond tool. It was established the follow main purposes of nanosized additives: change the chemical potential of interface between diamond and metallic binder result in alloying by chemically active nanoparticles; disperse strengthening the binder by involvement of nanoparticles inside of grains (hardness and toughness growing); involvement of nanoparticles on the grain boundaries (decrease the friction coefficient in cutting zone).
- *CRAPED* combining exothermic reaction with PED to deposit thick nanoparticles dispersive-strengthened coatings. Theoretical model of *CRAPED* was proposed. Three groups of nanostructured electrode materials for *CRAPED* were developed: dispersive-hardening ceramic materials with effect of simultaneous strengthening of carbide grains and metallic binder result in precipitations; nanoparticles disperse-strengthened composite materials with modified structure produced using focused alloying by nanoparticles which are modifiers affected to structure formation through the liquid phase and lock the recrystallization; nanostructured cemented carbides;
- Multicomponent multifunctional (wear-corrosion- and heat-resistant) nanostructured thin films and coatings deposited by PVD using *SHS*-composite targets were developed. Nanostructured thin film in system Ti-Al-B-N with extremely small crystallites less than 1 nm was observed. Multifunctional bioactive nanostructured films (Ti,Ta,Zr)-(Ca,P,Si)-(C,N,O) for load-bearing metallic implants has been developed. Multilayer high reactive ability films and foils for thermal generator were proposed.

### 3 Recent Results in Surface Engineering

#### 3.1 SHS-Composite Targets for PVD

Self-propagating high-temperature synthesis (*SHS*) is an alternative method, which provides a highly dense, uniform structure that exhibits required mechanical,

thermal, and electrical properties needed for such composite PVD target materials. The control of chemical composition of the targets facilitates the deposition of multicomponent films with required composition. The principal difference between sputtering of composite targets and metallic or intermetallic targets is that, in the first case, the multicomponent uniform flow of both metal and non metal atoms and ions is realized from the target to substrate. *SHS* composite targets can be especially benefit for the deposition of multifunctional nanostructured thin films and coatings in which both metallic (Cr, Al, Ca, Ti, Ta, Zr, others) and nonmetallic (C, N, O, B, Si, P) elements are present. As has recently been shown, the process of sputtering of multicomponent targets can be more complicated than sputtering from single element targets due to either the preferential sputtering effect or target poisoning. During the last decade various *SHS* composite targets have been developed and synthesized for deposition of hard tribological films and biological films. In order to enhance the toughness and thermal-resistance (resistance to thermal-cycling during high-power magnetron sputtering) needed for PVD targets, functionally graded targets have been developed and manufactured. As an example, *Figure 1* shows three layers functionally graded target with

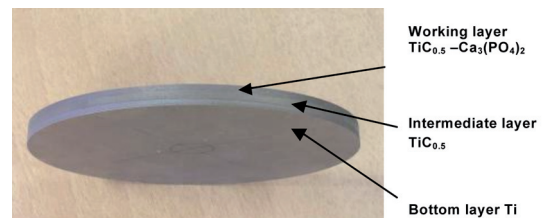


Fig. 1: Functionally graded target for the deposition of bio coatings

Ti<sub>0.5</sub>+Ca<sub>3</sub>(PO<sub>4</sub>)<sub>2</sub> working layer, Ti<sub>0.5</sub> intermediate layer, and titanium bottom layer as applied to deposition of biocompatible bioactive films.

#### 3.2 Hard Tribological Films

Tribological coatings are expected to demonstrate superior performance under severe cutting, stamping, and bearing conditions, being also resistant against humidity, corrosive environments, and temperature fluctuations. The desired properties can be achieved in

hard coatings based on carbides, borides, and nitrides of transition metals by complex alloying with other elements such as aluminium, chromium or silicon.

A comparative investigation of thermal stability, corrosion and oxidation resistance of Ti-B-N, Ti-B-N-xCr, Ti-B-N-xSi, and Ti-B-N-x(Al,Si) films ( $x = 11\text{--}14$  at%) deposited by DC magnetron sputtering and ion implantation assisted magnetron sputtering of composite targets Ti-B-N, Ti-Cr-B, Ti-Si-B, and Ti-Al-Si-B in a gaseous mixture of Ar+N<sub>2</sub> has been recently presented [1–3].

The films showed either a cubic B1 NaCl-type structure (Ti-B-N and Ti-Cr-B-N) or a hexagonal close-packed (hcp) AlB<sub>2</sub>-type structure without texture (Ti-Si-B-N and Ti-Al-Si-B-N). The films were characterized by a very small crystallite size in the range of 1 to 2 nm (Ti-Cr-B-N, Ti-Si-B-N, Ti-Al-Si-B-N) or 2 to 4 nm (Ti-B-N). For all films deposited on silicon substrate, the crystallite size remained stable up to 800 °C (Fig. 2a). At an annealing temperature of 1000 °C, the crystallite size slightly increased to 4 to 5 nm. However, upon annealing in the temperature range of 800 to 1000 °C, the crystallite size of Ti-Si-B-N and Ti-Al-Si-B-N films deposited on nickel substrate rapidly increased (Fig. 2b). The somewhat lower thermal stability of the multicomponent nanostructured films deposited on nickel substrate was caused by the diffusion of nickel from the substrate into the film. Nevertheless, a threshold temperature for recrystallization depends on the film structure. Films with fcc structure acted as a diffusion barrier for nickel diffusion from substrate up to 800 °C. For films with hcp structure the onset of recrystallization was much lower, 800 °C for the Ti-Al-Si-B-N films and 600 °C for the Ti-Si-B-N films, due to the fast diffusion of nickel atoms between the basal planes of hcp structure.

Upon annealing at 800 °C, the hardness increased up to 35 GPa (Ti-Cr-B-N films) and 41 GPa (Ti-B-N films) (Fig. 2c). These peaks of hardness after annealing at 800 °C were observed without substantial compromise in friction coefficient and wear rate. Both Raman and IR spectra of the as-deposited Ti-Cr-B-N film and the film annealed at 800 °C were quite similar. The changes observed in the spectra could be attributed to precipitation of h-BN, slight increase in grain size, decrease in nitrogen deficiency, and relaxation of compressive stress in the film. These can

be taken as indications of short-range diffusion and elements redistribution between the neighbor phases. As a result, the lattice parameter of the Ti-B-N and Ti-Cr-B-N films decreased to a value typical for TiN (Fig. 2d). Although the stress was changed from compressive to tensile (Fig. 2e), the crystallite size and hardness of the films deposited on silicon substrate remained relatively stable after annealing up to 800 to 1000 °C.

The oxidation stability of the Ti-B-N film was better than that of Ti-Si-B-N and TiN, but much lower than that of Ti-Cr-B-N and Ti-Al-Si-B-N films for which no traces of crystalline TiO<sub>2</sub> phase were observed after oxidation at 600 and 700 °C [2]. The formation of aluminum, silicon and bor rich oxide layers was shown to prevent films from further oxidation. After annealing at 900 °C, the Ti-Cr-B-N and Ti-Al-Si-B-N films formed several oxidation layers [4]. Top layers were mainly consisted by TiO<sub>2</sub> and Cr<sub>2</sub>O<sub>3</sub> for Ti-Cr-B-N and by TiO<sub>2</sub> and Al<sub>2</sub>O<sub>3</sub> for Ti-Al-Si-B-N. In lower layers fcc-TiN phase was present.

The steady-state friction coefficient of films against WC-Co counterpart materials was recorded to be 0.5 (Ti-B-N), 0.45 to 0.52 (Ti-Cr-B-N), and 0.4 to 0.5 (Ti-Si-B-N and Ti-Al-Si-B-N). It is worth noting that a comparison of Ti-Cr-B-N films with other hard tribological films tested under similar conditions shows a noticeable advantage from the view point of the wear resistance (Tab. 1).

The influence of chromium content on the structure and chemical, mechanical, and tribological properties of Ti-Cr-B-N films was studied by Shtansky et al. [3]. It was shown that with increasing chromium content, the Ti-Cr-B-N films have improved adhesion strength

**Tab. 1: Wear resistance of various films**

Film	Wear rate ( $\cdot 10^{-7}$ mm <sup>3</sup> /Nm)	Reference
Ti-Cr-B-N	1.8–4.1	[3]
Ti-B-N	300–450	[5]
Ti-C-N	4–34	[6]
Ti-Al-N	15–25	[7]
Ti-Al-B-N	10–150	[5]
Ti-B-C-N	50–80	[8,9]
Ti-W-B-C-N	10–15	[8]

and oxidation resistance up to 900 °C, whereas their hardness decreases.

Electrochemical tests also demonstrated the advantage of chromium-doped Ti-B-N films over the Ti-B-N, Ti-Si-B-N, and Ti-Al-Si-B-N films in the 1N H<sub>2</sub>SO<sub>4</sub> solution [2, 3]. The Ti-Cr-B-N films showed a more positive value of corrosion potential with respect to the Ti-B-N film and a four-fold decrease in the current density at a potential of passivation.

In contrast, for the Ti-Si-B-N and Ti-Al-Si-B-N films the corrosion and passive behaviors were rather negative. The current densities for the Ti-Si-B-N and Ti-Al-Si-B-N films under the passive conditions were 6.6 and 14 times higher and the corrosion potentials more negative than those for the Ti-B-N film. Thus adding chromium in the Ti-B-N film results in the stabilization of oxide layer on the top of the film under anodic polarization conditions.

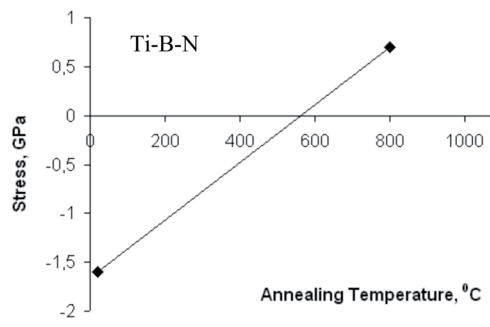
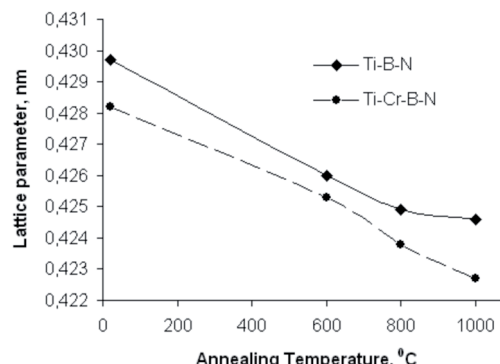
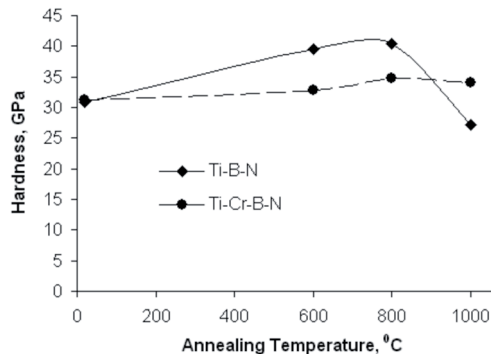
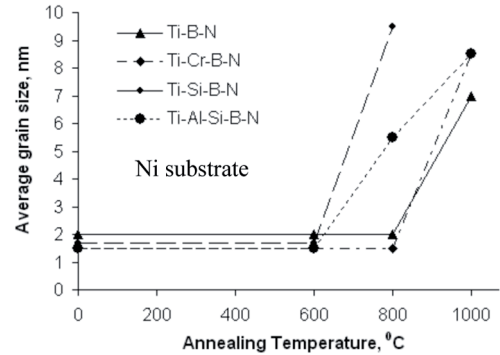
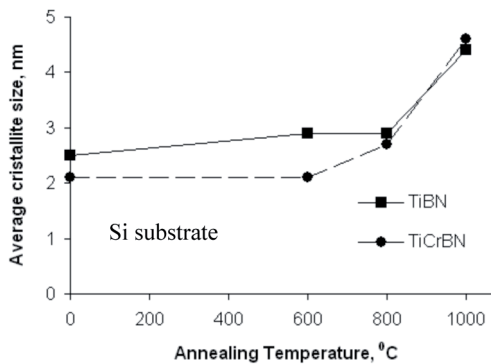


Fig. 2: Average grain size (a), (b), hardness (c), lattice parameter (d), and stresses in the films before and after annealing (e)

High-temperature thermal stability, corrosion- and oxidation resistance of hard tribological films may be of great importance for high-speed and dry cutting applications. The lifetime of drills with Ti-Cr-B-N and Ti-Si-B-N films against 12X18H10T steel increased, while drilling time of one hole decreased in comparison with uncoated high-speed tool and tool with TiN film. Comparison of lifetime of coated WC-Co mills and blades during milling and turning of D2 (Cr12MoV) and 321 (Cr18Ni10MnTi) steels respectively is shown in Figure 3. Tools with films showed superior characteristics in comparison with uncoated tools and tools with TiN film.

The SHS targets based on the MAX-phases  $Ti_{2-x}Cr_xAlC$  (where  $x = 0, 0.5, 1.5, \text{ and } 2$ ) can be successfully used to deposit nanostructured TiAlC(N), TiCrAlC(N), and CrAlC(N) coatings with enhanced characteristics, such as high hardness, low wear and friction, high thermal stability, oxidation and corrosion resistance [10]. The most important results can be summarized as follows. The coating growth rate increased when chromium content in the target was raised. The coatings had lower aluminum concentration and aluminum/chromium ratio compared with those of targets used.

With increased chromium content, the structure of as-deposited coatings changed from cubic to mixed structure consisting of cubic and hexagonal phases. The MAX-phase  $Cr_2AlC$  was observed to crystallize in the TiCrAlC coating ( $Ti_{0.5}Cr_{1.5}AlC$  target, hereafter denoted as  $x = 1.5$ ) deposited at a relatively low substrate temperature of 300 °C and high substrate bias voltage of -250 V. The as-deposited TiAlC

and TiCrAlC ( $x = 0.5$ ) coatings showed maximum hardness of 31 to 35 GPa. The TiAlC coating also demonstrated stable low friction coefficient against WC-Co in the range of 0.15 to 0.25. For coatings with high chromium content deposited in Ar+N<sub>2</sub>, the hardness was well below 24 GPa and the steady-state friction coefficient values were in the range of 0.5 to 0.65.

The TiAlC and TiCrAlC ( $x = 1.5$ ) coatings showed the best thermal stability as far as phase transformation is concerned. Their cubic structure was stable in the temperature range of 20 to 1200 °C, while the structure of the CrAlC coating underwent phase transformation upon annealing. The grain size of the nanocomposite TiAlC coating only slightly increased upon annealing up to 1200 °C. In the case of the TiCrAlC coating ( $x = 1.5$ ), the grain size did not change after heat treatment at 800 °C but rapidly increased with further heating. The CrAlC coating showed an increase in the grain size already after annealing at 800 °C.

Upon annealing, the hardness of the TiCrAlC ( $x = 0.5$ ) and CrAlC coatings decreased. The hardness of the TiCrAlC coating ( $x = 1.5$ ) increased from 25 GPa to 38 GPa reaching maximum value at 800 °C and then sharply decreased. The hardness of the TiAlC coating only slightly decreased from 31 to 25 GPa and retained constant up to 1200 °C.

The TiCrAlC ( $x = 1.5$ ) and CrAlC coatings with high chromium content were more oxidation resistant and demonstrated better electrochemical behavior compared to the TiCrAlC ( $x = 0.5$ ) and TiAlC coatings. The oxidation process was accompanied by a loss of nitrogen and diffusion of aluminum to the

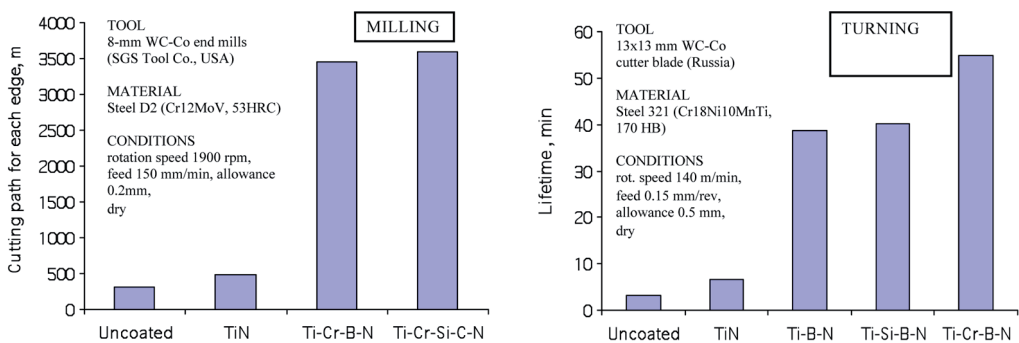


Fig. 3: Comparison of lifetime of coated and uncoated tools in dry (a) milling and (b) turning operations against Cr12MoV and Cr18Ni10MnTi steels

surface of coatings resulting in the formation of a layered structure consisting of  $\text{Cr}_2\text{O}_3$ ,  $\text{Al}_2\text{O}_3$ ,  $\text{Cr}_7\text{C}_3$ , and  $\text{AlN}_x\text{O}_y$  sublayers from the top to deep of the coating. The formation of aluminum-rich oxide layers prevented the TiCrAlCN and CrAlCN coatings from further oxidation.

Comparison of lifetimes of coated and uncoated 8 mm diameter WC-Co end mills (SGS Tool Company, USA) in dry milling of chromium steel (X12BF brand mark, 52-53 HRC) is shown in Figure 4.

The performance of the TiAlCN and CrAlCN coatings was compared with that of a commercial TiN coating which was used as reference. The milling tests were carried out on a drill-milling machine VF-1 (Haas, USA) under a rotation speed 1900 rev/min, feeding rate 150 mm/min, and allowance 0.2 mm. It can be seen that the lifetimes of end mills with TiAlCN and CrAlCN coatings were increased 2.5 to 3.5 and 1.7 to 2.4 times in comparison with uncoated tools and tools with TiN coating, respectively. Since the operation temperatures during milling did not appear to exceed 800 °C, which can be concluded from the absence of the coating color loss, the superior milling performance of the TiAlCN coating compared to the CrAlCN coating can be attributed to its better mechanical (high hardness) and tribological (low friction) properties. Low friction coefficient implies both decreased friction between the tool and chip in dry machining and reduced tendency to sticking and material pick up from the counterpart material which leads to the extended service life of cutting tools.

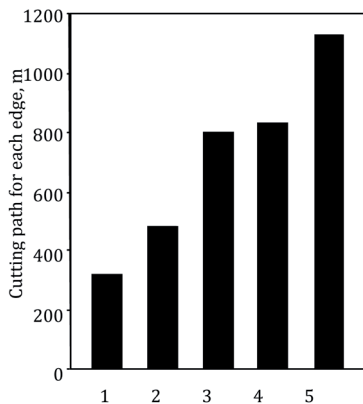


Fig. 4: Comparison of lifetimes of (1) uncoated cemented carbide mills and tools with (2) TiN, (3) CrAlCN, (4) TiCrAlCN ( $x = 0.5$ ), and (5) TiAlCN coatings

### 3.3 Nanocomposite Films with Improved Lubrication

Reduction of friction remains the main challenge for hard wear-resistant films. This is particularly true for films that work in aggressive environments and under the high temperature conditions. Solid lubricants such as dichalcogenides of transition metals of group VI are commonly used to decrease friction. As a solid lubricant, the  $\text{WSe}_x$  phase has an obvious advantage over other transition metal dichalcogenides due to its very narrow stoichiometric range  $1.97 < x < 2$ , making this phase more resistant against oxygen penetration. As a result, the  $\text{WSe}_2$  films showed superior performance both in air and under water [11].

Single-layer (SL) and multilayer (ML) TiCrBN/ $\text{WSe}_x$  films were deposited by ion implantation assisted sputtering of TiCrB and  $\text{WSe}_2$  targets [44]. The SL TiCrBN/ $\text{WSe}_x$  film consisted of mixture of fcc TiCrBN,  $\text{WSe}_2$ , and a- $\text{WSe}_x$  phases. The ML TiCrBN/ $\text{WSe}_x$  film consisted of a sequence of nanocrystalline TiCrBN and a- $\text{WSe}_x$  layers with thickness 85 to 110 and 11 to 17 nm, respectively.

The SL TiCrBN/ $\text{WSe}_x$  films showed almost the same hardness of 30 GPa as the TiCrBN film. The incorporation of  $\text{WSe}_x$  into TiCrBN film was shown to decrease the friction coefficient in air from 0.5 to 0.2 to 0.25 with only little influence on the wear resistance. In the case of SL TiCrBN/ $\text{WSe}_x$  films, the friction curves were typically flat with a very short running-in stage which did not exceed 50 m, whereas in the case of ML films, the fluctuations and spikes of friction coefficient were observed indicating that the transfer layer was not stable (Fig. 5a).

This was probably caused either by discrete re-supply of solid lubricant from under-layers into the friction contact or/and by periodical detachment of the wear debris. Analysis of the wear track morphology revealed smeared regions inside the tracks indicating the formation of tribofilms at the sliding interface and the volume fraction of smeared regions increased as the tribological test proceeded (Fig. 5b). It has been confirmed by Raman spectroscopy that the existence of  $\text{WSe}_2$  phase in sliding contact during the total period of the tribological test provides low friction. There were structural changes in the bulk of the film due to the surface oxidation process under the friction contact, but the  $\text{WSe}_2$  hexagonal planes were not destroyed by oxidation. The transition layer con-

taining  $WSe_2$ ,  $a-TiO_x$ , and  $a-WO_x$  phases was formed at the bottom of wear track and remained strongly adhered to the surface. The  $WO_x$  phase appeared to form due to oxidation and transfer of the ball material. The level of wear rate of the SL TiCrBN/ $WSe_x$  films was comparable to the wear rate of hard tribological films [3].

After annealing of the SL TiCrBN/ $WSe_x$  film at  $550\text{ }^\circ\text{C}$  for 1 h, the friction coefficient decreased further down to 0.2 and remained stable for 104 cycles (1 km) until the testing was stopped (Fig. 5a). The superior performance of the SL TiCrBN/ $WSe_x$  film after annealing can be explained by the presence of two constituents, of which one is a hard and high-temperature oxidation resistant (Ti,Cr)(B,N) phase with a grain size of a few nanometers and the other is a mixture of  $WSe_2+a-WSe_x$  solid lubricant grains and

inter-granular phases. The choice of the hard constituent can be critical. As was shown previously, the TiCrBN films possess improved oxidation resistance up to  $900\text{ }^\circ\text{C}$  [3].

The electrochemical tests demonstrated that the open-circuit corrosion potentials of the SL and ML TiCrBN/ $WSe_x$  films had positive values in the range of 0.22 to 0.3 V, which correspond to passive state [12]. Incorporation of  $WSe_x$  into TiCrBN film does not significantly affect the passive state of the film under anodic polarization conditions.

### 3.4 Multifunctional Bioactive Nanostructured Films

In order to obtain artificial implants with enhanced physical, chemical, mechanical, tribological, and biological properties resulting in their accelerated self-adaptation in human body and long-term performance, it is necessary to combine the advantages of materials with various properties: biocompatibility, bioactivity, excellent corrosion resistance, high fatigue and bending strength, low modulus of elasticity and friction coefficient, high wear resistance.

One of the possible solutions to the problem of producing load-bearing implants is to coat a film with multifunctional properties. A new approach to design perspective multifunctional bioactive nanostructured films (MuBiNaFs) for load-bearing metallic implants has been developed [13–18]. MuBiNaFs were deposited by magnetron sputtering of composite targets  $Ti_{0.5}+X$  and  $(Ti,Ta)C+X$  (where  $X = CaO, TiO_2, Ca_{10}(PO_4)_6(OH)_2, ZrO_2, Si_3N_4,$  and  $Ca_3(PO_4)_2$ ) in an argon atmosphere or reactively in a gaseous mixture of  $Ar+N_2$ . The application of the ion implantation assisted magnetron sputtering (IIAMS) of SHS-composite targets offers a flexible approach to surface improvement of metal implants. This technique facilitates in the production of dense, well adhered films with controlled elemental composition.

A comparison of MuBiNaFs with the properties of bulk materials (metals and alloys, ceramics) and thin films produced by alternative methods shows a noticeable advantage from the view point of the whole combination of physical, mechanical, tribological, and biological properties.

The MuBiNaFs revealed a high level of bioactivity due to their nanocomposite structure with various functional groups on the surfaces. For instance, the

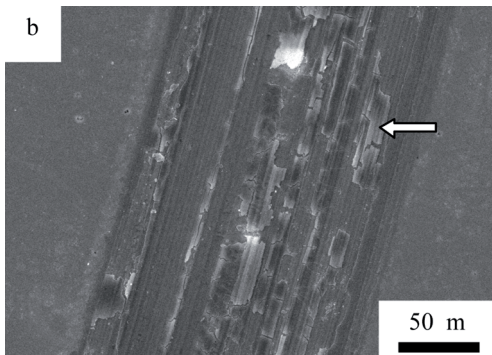
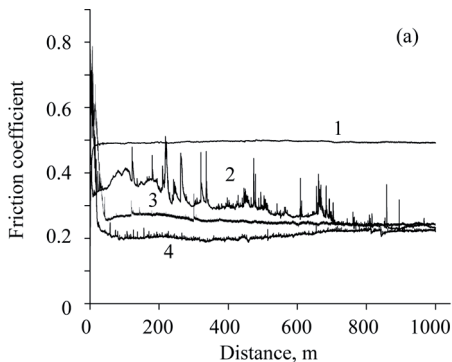


Fig. 5: Friction coefficient of the films(a); (1) TiCrBN; (2) ML TiCrBN/ $WSe_x$ ; (3) SL TiCrBN/ $WSe_x$  film; (4) the same as (3) but after annealing at  $550\text{ }^\circ\text{C}$  for 1 h; Micrographs of the wear tracks of SL TiCrBN/ $WSe_x$  film after the sliding distance of 1000 m (b). Smearing region is shown by arrow [12]

films deposited in an argon atmosphere consisted of (Ti,Ta)C, Ti<sub>x</sub>O<sub>y</sub>, and CaO phases in an amorphous matrix with P-O, C-O, and O-H bonding. In the films deposited in a gaseous mixture of Ar+N<sub>2</sub>, apart from the (Ti,Ta)(C,N), Ti<sub>x</sub>O<sub>y</sub>, and CaO phases, the indication of diamond-like carbon, metallic tantalum and traces of P-O bonding were observed [13].

As shown in *Table 2*, the MuBiNaFs are characterized by high hardness (H), reduced Young's modulus (E), high percentage of elastic recovery, high resistance to plastic deformation (described by the ratio H3/E2), and long elastic strain to failure (described by the ratio H/E). The last parameter is an indicator of film durability and wear resistance. As a hard tissue replacement, films with the low elastic modulus are particularly beneficial, especially if E can be adjusted to closely match that of the underlying substrate material (stainless steel, NiA, CoA, Ti) in order to minimize film/substrate interfacial stress and because the smaller elastic modulus can result in smaller stress shielding. Low Young's modulus also allows better transfer of functional loads to bone.

The MuBiNaFs showed stable low friction coefficient in the range of 0.2 to 0.25 both in air and under physiological solution which is significantly lower than those of TiC and TiN films. The wear rate of the MuBiNaFs was two orders of magnitude lower than that of titanium substrate both in ambient air and under physiological solution. No noticeable wear of counterpart material was registered in both cases. The films have low dissolution rate under physiologi-

cal solution and therefore are suitable for orthopedic and dental applications.

In general, interfacial failure is one of the most predominant failure modes of coated implants. Resistance of various film/substrate systems to scratching was recently studied [15, 19]. It was shown that the resistance of film/substrate systems to scratching depends on the combination of elastic and plastic properties of both the film and substrate. From scratch tests, it can be concluded that the adhesion strength is high because the films deform either elastically or plastically without detaching from substrate until high critical load was achieved.

Fatigue tests (bending with rotation) demonstrated that the fatigue limit of titanium rods, 7.5 mm in diameter, with Ti-Ca-C-O-N films was close to 350 MPa similar to that of titanium sample without the film.

Contact angle measurements indicated hydrophilic nature of MuBiNaF surfaces. The electrochemical tests demonstrated that all MuBiNaFs had positive values of corrosion potential with low current density. MuBiNaFs also showed more positive values of potential than titanium that promote titanium alloy passivation.

Zeta-potential measurements showed that the surface of all MuBiNaFs was negatively charged at pH values ranging from 4 to 10 and hence, could combine selectively with positively charged Ca<sup>2+</sup> ions in body fluid to form calcium based intermediate phases that may further transform into apatite, because apatite is the stable phase in body environment [17].

In vitro studies showed that cultured IAR-2 epitheliocytes, Rat-1 fibroblasts, and MC3T3-E1 osteoblastic cells were well spread on the surface of MuBiNaFs and their actin cytoskeleton was well organized. Osteoblastic cells had a high rate of proliferation on all examined films and expressed early-stage differentiation marker alkaline phosphatase. The MuBiNaFs revealed a high level of biocompatibility and biostability in the experiments in vivo. Implantation studies using rat calvarian and hip defect models indicated early signs of bone formation on coated titanium implants. After one month, a close contact between the implant surface and cortical bone was observed without any bone loss at the interface [15]. The results described above show that MuBiNaFs possess a combination of high hardness, fatigue and adhesion strength, reduced Young's modulus, low

**Tab. 2: Mechanical characteristics of MuBiNaFs in comparison with other biomedical materials**

Material	H (GPa)	E (GPa)	H/E	H3/E2 (GPa)
Al <sub>2</sub> O <sub>3</sub>	21	380	0.055	0.06
ZrO <sub>2</sub>	12	205	0.06	0.04
TiC	26	480	0.055	0.07
TiN	22	440	0.05	0.055
Co-based alloys	8.2	230	0.035	0.01
Ni-based alloys	8.0	170	0.05	0.02
TiNi	4.8	66	0.07	0.025
Ti-based alloys	4	120	0.03	0.04
440C steel	7	200	0.035	0.009
MuBiNaFs	23–40	230–350	0.1–0.15	0.2–0.9

wear and friction, high corrosion resistance with high level of biocompatibility, bioactivity, and biostability that makes MuBiNaFs promising candidates as protective films on the surface of metallic implants such as orthopedic prostheses, materials for connective surgery and dental implants.

### 3.5 CRAPED

The method of *CRAPED* utilizes an exothermic reaction initiated by electric discharge within an inter electrode space [20, 21]. In this case, the discharge energy  $Q_{el}$  must be comparable with (or greater than) the reaction heat  $Q_{ch}$ . The *TRESS* process can be carried out in the three modifications shown in *Figure 6*.

In the modification shown in *Figure 6* as *CRAPED 1*, an electrode filled with a reactive powder mixture acts as anode while a substrate, as cathode. During pulsed discharge, the powder material from the anode undergoes the exothermic chemical reaction  $\Sigma A_i + \Sigma B_j = Z + Q_{ch}$  within the inter electrode space. As

a result, reaction products  $Z$  are deposited onto the substrate surface. Due to formation of a transition joint at the coating/substrate interface, the deposited coating exhibits a high adhesion to the substrate.

In the modification shown as *CRAPED 2*, a copper electrode acts as cathode while a substrate, as anode. Reactive layer was deposited by brushing a suspension of a given powder in an aqueous solution of silicate glue. Pulsed discharge between the electrodes initiates local exothermic reaction whose products are then deposited as a coating.

In the modification *CRAPED 3* metal or composite (including nanostructured materials) or graphite electrode chemically reacted with substrate material.

In every case,  $\Sigma Q = Q_{el} + Q_{ch}$ . The fact that  $Q_{ch} \geq Q_{el}$  leads to an increase in the extent of conversion, release of thermal strains, and increase in the coating thickness.

For example, Ni-Al electrodes were used in the form of powder compacts, while Ti-B, Ti-C-Ni-Al, Ti-C-Al,

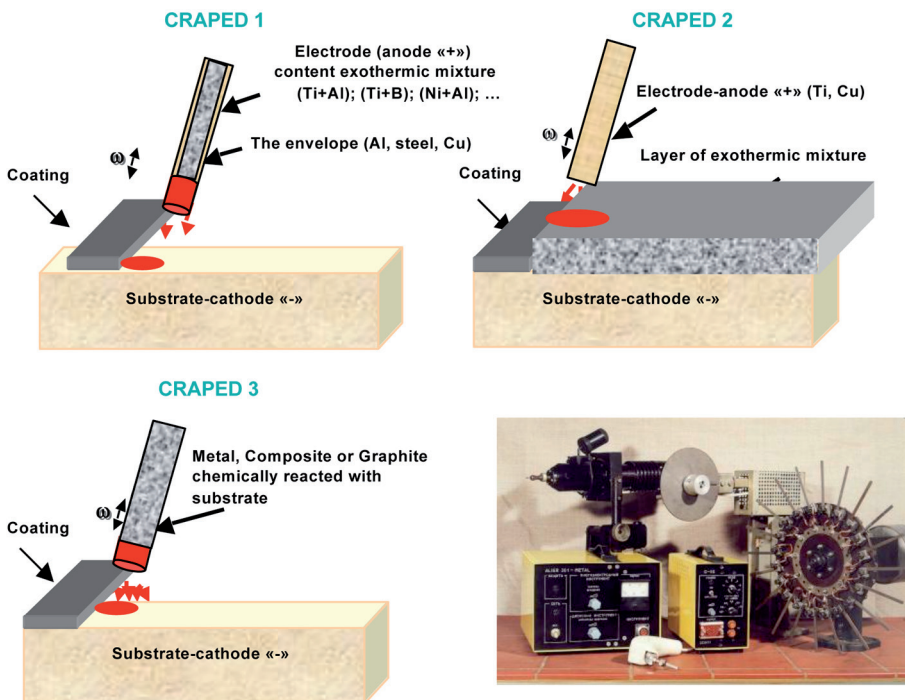


Fig. 6: Three modifications of the CRAPED

Ti-Al-diamond, and Ti-B-diamond electrodes were prepared by dragging the above powders into aluminum, steel, and copper shells. Ti-Si, Ti-Si<sub>3</sub>N<sub>4</sub>, Ni-Al-diamond, and Ti-Al-diamond mixtures were used to prepare the glued powder layers. Graphite or nanostructured cemented carbides anodes can be used in *CRAPED* 3. Titanium, nickel alloys and steel were used as substrates [22–25].

Structure, composition and properties of deposited coatings as well as the processes taking place at the electrode tip were investigated. Elucidated were the features of the deposition process onto different substrates. The weight gain of substrate was determined by high-speed filming of the process. Two models of the process have been suggested. The material of electrode shell was found to affect the properties of *CRAPED* coatings. At some critical pulse discharge energy ( $E_{cr}$ ), we observed the spontaneous ignition of electrode material or glued powder layer. Due to formation of TiB<sub>2</sub>, TiC, NiAl, TiAl, and Ti<sub>5</sub>Si<sub>3</sub> during the deposition process, the deposited multifunctional coatings were found to exhibit a higher hardness and heat/wear resistance as compared to those of substrate material. *CRAPED* coatings were found promising for subsequent deposition of diamond films by CVD [26, 27]. Compared to PED, the *CRAPED* process is more energy/cost-saving.

### 3.6 PED

Further advance in the *PED* technology requires the development of new process equipment and new electrode materials (EMs) that would ensure deposition of coatings with improved service parameters.

Nowadays, the electrospark modification of surfaces is carried out using WC-containing hard-alloy EMs of such brands as VK (WC-Co), TK (TiC-WC-Co), and TTK (TiC-WC-TaC-Co). Less popular are such W-free hard alloys as TN (TiC-Ni-Mo), KTN [Ti(CN)-Ni-Mo], LKTs [TiZr(CN)-Ni-Mo], etc. The drawbacks of the above alloys are (a) their high erosion resistance (hence low deposition rate) and (b) relatively low heat/corrosion resistance. As a result, the discharge energy is spent largely on the warm-up and local melting of anode material. This leads to a low carbide content of the coating and a high amount of binder. The ES coatings deposited with standard WC-containing electrodes normally exhibit low hardness and wear/heat resistance, high sur-

face roughness, high friction coefficient, and also the presence of discontinuities and defects. In this context, we have suggested a novel approach (other than powder metallurgy) to production of promising tungsten-free hard alloy EMs by *SHS*.

It was found that the addition of refractory nanosized additives into a starting *SHS* mixture markedly modifies the structure of *SHS* product (to be used as EM) and hence the service characteristics of the coating deposited with such electrodes onto different substrates (such as titanium and nickel alloys, steels).

The following *SHS*-produced hard alloys were used as a base of EMs: TiC-Cr<sub>3</sub>C<sub>2</sub>-Ni (STIM-3B), TiC-Ni (STIM-2), TiC-Ni alloy KhN70Yu (STIM-2/40NZh), TiC-NiAl (STIM-40NA), TiC-Ti<sub>3</sub>AlC<sub>2</sub> (STIM-40A), and TiB<sub>2</sub>-TiAl (STIM-9/20A), and others. Nanosized powders of ZrO<sub>2</sub>, Al<sub>2</sub>O<sub>3</sub>, NbC, Si<sub>3</sub>N<sub>4</sub>, W, Mo, WC, WC-Co, and diamond were added to a starting *SHS* mixture [28, 29].

We characterized the structure, composition, and properties of PED-coatings and investigated the effect of nanosized additives on the process of mass transfer and properties of deposited coatings. The PED-coatings deposited with dispersion-strengthened EMs exhibited elevated hardness, continuity, thickness, wear/heat resistance as well as a lower grain size, friction coefficient (Kfr), and surface roughness ( $R_a$ ,  $R_z$ ,  $R_{max}$ ). As is seen in *Figure 7*, the coatings deposited onto a titanium alloy with TiC-Ti<sub>3</sub>AlC<sub>2</sub> electrodes are formed by Ti(C,N) grains (70 to 500 nm in size) formed upon recrystallization of finer grains. Measured adhesion strength (critical load) of coatings to the substrate is a very high. Indentation (diamond indenter, F up to 130 N) of the coatings deposited onto a titanium alloy with TiC-NiAl-NbC nano electrodes did not display any signs for exfoliation/detachment of deposited material. The elastic recovery was found to have a value of 40 to 50 %. It has been demonstrated that the PED-coatings deposited with dispersion-strengthened EMs exhibit improved service parameters.

### References

- [1] D. V. Shtansky, A. N. Sheveiko, M. I. Petrzhik, Ph. V. Kiryukhantsev-Korneev, E. A. Levashov, A. Leyland et al.: Hard Tribological Ti-B-N, Ti-Cr-B-N, Ti-Si-B-N and Ti-Al-Si-B-N Films; *Surf Coat Technol* (2005);200:208-12
- [2] Ph. V. Kiryukhantsev-Korneev, D. V. Shtansky, M. I. Petrzhik, E. A. Levashov, B. N. Mavrin: Thermal stability and oxidation resistance of Ti-B-N, Ti-Cr-B-N, Ti-Si-B-N and Ti-Al-Si-B-N films; *Surf Coat Technol* (2007);2001:6143-47

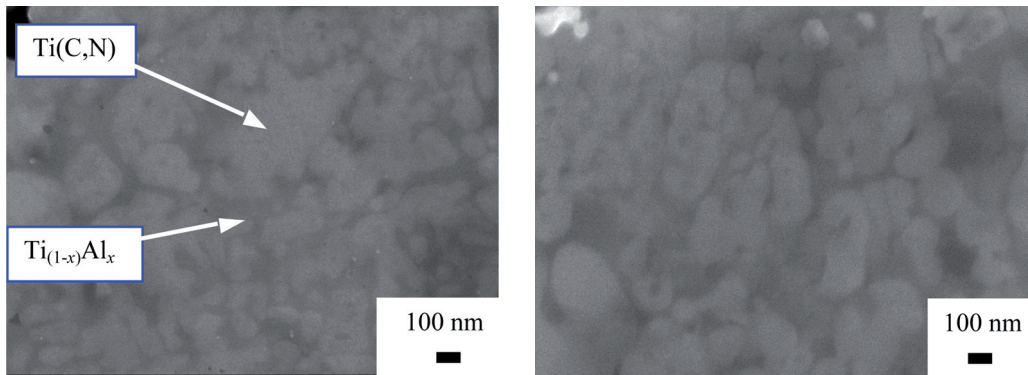


Fig. 7: Microstructure of the coatings deposited with  $TiC-Ti_3AlC_2-ZrO_2$  nano (a) and  $TiC-Ti_3AlC_2$  (b) electrodes onto a titanium alloy (OT4-1)

- [3] D. V. Shtansky, Ph. V. Kiryukhantsev-Korneev, A. N. Sheveiko, A. E. Kutryev, E. A. Levashov: Hard tribological Ti-Cr-B-N films with enhanced thermal stability, corrosion- and oxidation-resistance; *Surf Coat Technol* (2007);202:861-65
- [4] C. Paternoster, A. Fabrizi, R. Cecchini, S. Spigarelli, Ph. V. Kiryukhantsev-Korneev, A. Sheveiko: Thermal evolution and mechanical properties of hard Ti-Cr-B-N and Ti-Al-Si-B-N coatings; *Surf Coat Technol* (2008);203:736-40
- [5] C. Rebholz, H. Ziegele, A. Leyland, A. Matthews: Structure, mechanical and tribological properties of Ti-B-N and Ti-Al-B-N multiphase thin films produced by electron-beam evaporation; *J Vac Sci Technol A* (1998);16:2851-7
- [6] S. J. Bull, D. G. Bhat, M. H. Staia: Properties and performance of commercial TiCN films. Part 2: tribological performance; *Surf Coat Technol* (2003);163-164:507-14
- [7] K. Chu, P. W. Shum, Y. G. Shen: Substrate bias effects on mechanical and tribological properties of substitutional solid solution (Ti, Al)N films prepared by reactive magnetron sputtering; *Mater Sci Eng B* (2006);131:62-71
- [8] F. Kustas, B. Mishra, J. Zhou: Fabrication and characterization of  $Ti_2/TiC$  and tungsten co-sputtered wear films; *Surf Coat Technol* (2002);153:25-30
- [9] D. Zhong, E. Sutter, J. J. Moore, G. G. W. Mustoe, E. A. Levashov, J. Disam: Mechanical properties of Ti-B-C-N films deposited by magnetron sputtering; *Thin Solid Films* (2001);398-399:320-5
- [10] D. V. Shtansky, Ph. V. Kiryukhantsev-Korneev, A. N. Sheveiko, B. N. Mavrin, C. Rojas, A. Fernandez, E. A. Levashov: Comparative investigation of  $TiAlC(N)$ ,  $TiCrAlC(N)$ , and  $CrAlC(N)$  coatings deposited by sputtering of MAX-phase  $Ti_{2-x}Cr_xAlC$  targets; *Surface and Coatings Technology*, doi:10.1016/j.surfcoat.2009.05.036
- [11] D. V. Shtansky, T. A. Lobova, V. Yu. Fominski, S. A. Kulinich, I. V. Lyasotsky, M. I. Petrzhek, E. A. Levashov, J. J. Moore: Structure and tribological properties of  $WSe_x$ ,  $WSe_x/TiN$ ,  $WSe_x/TiCN$  and  $WSe_x/TiSiN$  films; *Surf Coat Technol* (2004);183:328-36
- [12] D. V. Shtansky, A. N. Sheveiko, D. I. Sorokin, L. C. Lev, B. N. Mavrin, Ph. V. Kiryukhantsev-Korneev: Structure and properties of multi-component and multilayer  $TiCrBN/WSe_x$  films deposited by sputtering of  $TiCrB$  and  $WSe_x$  targets; *Surf Coat Technol* (2008);202:5953-61
- [13] D. V. Shtansky, N. A. Gloushankova, I. A. Bashkova, M. A. Kharitonova, T. G. Moizhess, A. N. Sheveiko et al.: Ta-doped multifunctional bioactive nanostructured films; *Surf Coat Technol* (2008);202:3615-24
- [14] D. V. Shtansky, N. A. Gloushankova, I. A. Bashkova, M. I. Petrzhek, A. N. Sheveiko, Ph. V. Kiryukhantsev-Korneev et al.: Multifunctional Biocompatible Nanostructured Films for Load-Bearing Implants; *Surf Coat Technol* (2006);201:4111-18
- [15] D. V. Shtansky, N. A. Gloushankova, I. A. Bashkova, M. A. Kharitonova, T. G. Moizhess, E. A. Levashov et al.: Multifunctional Ti-(Ca,Zr)-(C,N,O,P) films for load-bearing implants; *Biomaterials* (2006);27:3519-31
- [16] D. V. Shtansky, N. A. Gloushankova, A. N. Sheveiko, M. A. Kharitonova, T. G. Moizhess, E. A. Levashov, F. Rossi: Design, characterization and testing of TiC-based multicomponent films for load-bearing biomedical applications; *Biomaterials* (2005);26:2909-24
- [17] D. V. Shtansky, E. A. Levashov, N. A. Gloushankova, N. B. D'yakonova, S. A. Kulinich, M. I. Petrzhek, F. V. Kiryukhantsev-Korneev, F. Rossi: Structure and properties of  $ZrO_2$  and CaO-doped  $TiC_xN_x$  films for biomedical applications; *Surf Coat Technol* (2004);182:101-11
- [18] D. V. Shtansky, I. A. Bashkova, E. A. Levashov, T. A. Chipysheva, Yu. M. Vasil'ev, N. A. Gloushankova: Multifunctional Nanostructural Films for Load-bearing Implants; *Dokl Biochem Biophys* (2005);404:336-8
- [19] D. V. Shtansky, M. I. Petrzhek, I. A. Bashkova, F. V. Kiryukhantsev-Korneev, A. N. Sheveiko, E. A. Levashov: Adhesion, friction, and deformation characteristics of Ti-(Ca,Zr)-(C,N,O,P) films for orthopedic and dental implants; *Phys Solid State* (2006);48(7):1301-8
- [19] E. A. Levashov, A. G. Nikolaev, A. S. Rogachev, A. E. Kudryashov, M. Ohyanagi, M. Koizumi, and S. Hosomi: Electrode Material for the Deposition of Superabrasive Coatings and the Technique of Their Production; *Int. Patent WO99/18258* (October 3, 1997)
- [20] E. A. Levashov, A. E. Kudryashov, E. I. Kharlamov, M. Ohyanagi, M. Koizumi, S. Hosomi: Formation of FGM Coating by the New Method of Thermoreactive Electrospark Surface Strengthening (TRESS), in *Proceedings of 5th International Symposium on Functionally Graded Materials* (Dresden, Germany, October 26–29, 1998), Kaysser W. A., Ed., Switzerland: Trans Tech Publications, pp. 262–270
- [21] E. I. Kharlamov, A. E. Kudryashov, E. A. Levashov, M. Ohyanagi, S. Hosomi, M. Koizumi: Structure and Properties of Diamond-Containing TRESS-Coatings Produced Using New High Frequency Installation Alier-Metal; *Abstr. 6th Int. Symp. on Self-Propagating High-Temperature Synthesis*, Feb. 17–21, 2002, Haifa, Israel, p. 77
- [22] E. I. Zamulaeva, E. A. Levashov, A. E. Kudryashov, P. V. Vakaev, M. I. Petrzhek: Electrospark Coatings Deposited onto an Armco Iron Substrate with Nano- and Microstructured WC-Co Electrodes: Deposition Process, Structure, and Properties; *Surface and Coatings Technology* (2008), Vol. 202, p. 3715-3722
- [23] E. A. Levashov, E. I. Zamulaeva, A. E. Kudryashov, P. V. Vakaev, M. I. Petrzhek, A. Sanz: Materials Science and Technological Aspects of Electrospark Deposition of Nanostructured WC-Co Coatings onto Titanium Substrates; *Plasma Process and Polymers* (2007), No. 4, p. 293–300

- [24] E. A. Levashov, E. I. Zamulaeva, A. E. Kudryashov, P. V. Vakaev, T. A. Sviridova, M. I. Petrzlik: Mechanism of Deposition and Structure Formation of Electrospark Coatings onto a Nickel Substrate with Nano- and Microstructured WC-Co Electrodes; *Jahrbuch Oberflächentechnik*, Band 62 (2006), Bad Saulgau, Germany, p. 170–179
- [25] E. A. Levashov, P. V. Vakaev, E. I. Zamulaeva, A. E. Kudryashov, Yu. S. Pogozhev, D. V. Shtansky, A. A. Voevodin, A. Sanz: Nanoparticle dispersion-strengthened coatings and electrode materials for electrospark deposition; *Thin Solid Films* (2006), Vol. 515, p. 1161–1165
- [26] A. E. Kudryashov, E. I. Zamulaeva, P. V. Vakaev, E. A. Levashov, V. G. Ralchenko: The Structure and Properties of Coatings Produced by Thermoreactive Electrospark Surface Strengthening (TRESS); *Abstr. 8th Int. Symp. on Self-Propagating High-Temperature Synthesis*, Cagliari, Italy, 21–24 June, 2005, p. 95
- [27] A. Sanz, E. A. Levashov, D. V. Shtansky, A. E. Kudryashov: A Method for Deposition of Dispersion-Strengthened Coating and Composite Electrode Material for Deposition of Such Coatings; *Int. Patent WO 2008/014801*, (2008)
- [28] E. A. Levashov, P. V. Vakaev, E. I. Zamulaeva, A. E. Kudryashov, V. V. Kurbatkina, D. V. Stansky, A. A. Voevodin, A. Sanz: Disperse-Strengthening by Nanoparticles Advanced Tribological Coatings and Electrode Materials for their Deposition; *Surface and Coatings Technology* (2007), vol. 201, pp. 6176–6181
- [29] E. A. Levashov, A. E. Kudryashov, P. V. Vakaev: Prospects of Nanodispersive Powder Applications in Surface Engineering Technologies; in a book: *Nanostructured Thin Films and Nanodispersion Strengthened Coatings* by A. A. Voevodin, D. V. Shtansky, E. A. Levashov, J. J. Moore, Eds., Amsterdam: Kluwer, 2004, pp. 231–240